Original Article

Ultrastructural Study of Rat Testis Following Conventional Phototherapy during Neonatal Period

Hare Krishna, Asha Changil[1], M. Srinivas[2], Tara Sankar Roy, Tony George Jacob

Department of Anatomy, All India Institute of Medical Sciences, [1]Department of Anatomy, Army College of Medical Sciences, New Delhi, [2]Department of Paediatric Surgery, ESIC Medical College, Hyderabad, Telangana, India

Abstract

Introduction: Phototherapy is the most common treatment for neonatal jaundice. This study sought to determine ultrastructural changes in testis, at different time-points, after 48 hours of conventional phototherapy was given to newborn rats. **Methods:** Newborn male Wistar rats ($n = 36$) were divided into two groups as follows – group 1 (G1), control (without phototherapy) and group 2 (G2), exposure to conventional phototherapy for 48 h. Six animals from each group were sacrificed on postnatal days (PND) 70, 100 and 130. The testes were dissected out and processed for Transmission Electron Microscopy (TEM). **Results:** TEM showed that G2 on PND 70 and 100 showed damaged organelles, including nuclei, mitochondria, endoplasmic reticulum, vacuoles and electron dense bodies in the testes. Seminiferous Tubule on PND130 showed lesser damage. On PND70 ST wall thickness (STWT) of G2 was significantly higher ($P < 0.001$) than G1 STWT of G2 was significantly lower than G1 on PND100 ($P = 0.047$) and on PND130 ($P < 0.001$). Mitochondrial diameter in spermatogonia was significantly higher in G2 on PND70 ($P = 0.001$), PND100 ($P = 0.031$) and PND130 ($P = 0.028$). Primary spermatocytes in G2 also had larger mitochondria on PND70 ($P < 0.001$), PND100 ($P = 0.007$) and PND130 ($P = 0.008$). Further, spermatids had larger mitochondria in G2 on PND70 ($P < 0.001$), PND100 ($P = 0.044$) and PND130 ($P < 0.001$). **Conclusion:** Phototherapy causes degenerative changes in rat testis on PND70 and 100 that partially recover by PND 130.

Keywords: Mitochondria, neonatal jaundice, seminiferous tubule, spermatocyte, spermatogonium, transmission electron microscopy

Introduction

About 60% of normal newborns become jaundiced during their 1st week of life.[1] In most of the cases, hyperbilirubinemia remains undetected due to early discharge of newborn infants which is the leading cause of readmission of newborns to hospital.[2] High levels of bilirubin can lead (Pb) to bilirubin encephalopathy, which produces irreversible brain damage,[3] if the treatment is not given properly and immediately. Phototherapy (PT) is the most common treatment for neonatal hyperbilirubinemia[4] due to its noninvasive nature, simple, more economic, and most of the reversible side effects.[5] However, PT has a few adverse effects such as diarrhea, skin eruptions, dehydration, patent ductus arteriosus, retinal damage, and bronze-baby syndrome[6,7] Equivalent exposure of mouse lymphoma cell lines to light was seen to increase apoptosis in them[8] and *in vivo* the same was seen in the small intestine of the neonatal rat.[9] Conventional PT is given to neonates by completely exposing them to light in an incubator. The thin skin of the neonate may predispose the testes to phototoxicity. The rat pup is known to attain sexual maturity by postnatal day (PND) PND70.[10] Although at birth, the rat testes are intra-abdominal, the pup is born nude (lacks fur and has very thin skin), the exposure to PT may primarily or secondarily affect the internal organs.[6] Very little is known about the potential long-term side effects of PT on the testes, though the effects may be seen much later in life as infertility of the individual. Further, these changes may be subtle and unapparent on conventional light microscopy.[6] Therefore, the present study was aimed at investigating the ultrastructural changes in the testis of rat pups that had been given conventional PT, on PNDs 70, 100, and 130.

Access this article online

Quick Response Code:

Website: http://www.jmau.org/

DOI: 10.4103/JMAU.JMAU_17_18

Address for correspondence: Dr. Tony George Jacob, Department of Anatomy, All India Institute of Medical Sciences, New Delhi - 110 029, India.
E-mail: tonygeorgejacob@gmail.com

How to cite this article: Krishna H, Changil A, Srinivas M, Roy TS, Jacob TG. Ultrastructural study of rat testis following conventional phototherapy during neonatal period. J Microsc Ultrastruct 2018;6:205-11.

Materials and Methods

After obtaining clearance from the Institutional Animal Ethics Committee, the present study was carried out on 36 male newborn Wistar rats. These animals were randomly divided into two groups. The first group of neonatal male pups (G1) with their respective dams were not exposed to conventional PT and served as controls. The second group (G2) of the same aged male pups and their dams were exposed to conventional PT for 48 h (Model PB 100, 3389, Phoenix Medical Systems Pvt. Ltd, Chennai, Tamil Nadu, India). After 48 h of continuous PT, these pups were kept in the cages with their dams until weaning (in rats it occurs at approximately 30th PND). Thereafter, they were kept in separate shoe-box cages and fed standard rodent chow with water ad libitum. During the study, all rats were housed in 12-h light/dark cycles in an ambient temperature that ranged from 20°C to 26°C and 30%–70% relative humidity. The pups grew normally to attain 70, 100, and 130 PNDs of age. Thereafter, they were sacrificed by lethal anesthesia and perfused first with normal saline and then with chilled 4% phosphate-buffered paraformaldehyde (pH 7.4), and the testes were dissected out.

For transmission electron microscopy (TEM), small pieces of the testis were cut and fixed in 2.5% glutaraldehyde and 2% paraformaldehyde in 0.1 M phosphate buffer (PB) (pH 7.3) for 12 h at 4°C. Thereafter, the tissues were washed in 0.1M PB and secondarily fixed in 1% OsO_4 for an hour at 40°C. The samples were dehydrated in ascending grades of acetone, infiltrated, and embedded in araldite CY 212 (TAAB, UK). Sections of 1 μm thickness were cut on an ultramicrotome, (Leica EM UC7, Leica Microsystems, Austria) mounted on to glass slides, stained with aqueous toluidine blue and observed under a light microscope to identify the area of interest for TEM. Thereafter, ultrathin sections (70–80 nm, silver to gold sections) were cut and stained with alcoholic uranyl acetate and alkaline Pb citrate and observed under a Morgagni 268D TEM (FEI Company, the Netherlands) at an operating voltage 80 kV. Images were digitally acquired by a CCD camera (Megaview III, FEI Company) using iTEM software (Soft Imaging System, Münster, Germany) attached to the microscope. In addition, the images were analyzed on Image-J software (NIH), after calibration per image. We studied two sections for each rat. We measured the thickness of the basement membrane (BM) of the seminiferous tubules (STs) on 119 sites in G1 and 180 sites in G2, distributed, almost equally, among all six animals in each group. We also measured the maximal diameters of the mitochondria in spermatogonia (Sg) (64 mitochondria in G1 and 63 mitochondria in G2), primary spermatocytes (PSp) (133 mitochondria in G1 and 120 mitochondria in G2) and spermatids (Sd) (732 mitochondria in G1 and 959 mitochondria in G2). Here too, the sites were distributed equitably among all six animals of each group.

The different cells of the STs were identified by the features already described.[11] Sg lie on the BM and have rounded euchromatic nuclei and peripheral heterochromatin [Figures 1 and 2a]. PSp appears as large, rounded cells, with large spherical nuclei containing clumps of heterochromatin scattered all over the nucleoplasm, lying near the BM of the tubule above the Sg [Figures 1 and 3a]. Sd are identified by their electron-dense acrosomal cap (AC) on one side of the nucleus. Their nuclei are rounded and have euchromatic nuclei with evenly distributed chromatin. The cytoplasm has a prominent Golgi apparatus and peripherally arranged mitochondria [Figures 1 and 4a]. Sertoli cells have large, indented, euchromatic nuclei with prominent nucleoli located close to the basal lamina. Their cytoplasm shows abundant mitochondria and smooth ER (SER) [Figure 5a]. Mitochondria are cytoplasmic double-membrane bound organelle that has their inner membrane thrown into folds called cristae. The SER is made of a network of flattened membrane-bound sacs and tubules. The membrane forming the SER may be continuous with the nuclear membrane.

In addition, there are flattened myoid cells that cover the STs and are part of the ST wall (STW) [Figure 2a].

Statistical analysis

The data were first analyzed for normal distribution using a kurtosis plot. The numerical data were then summarized as arithmetic mean ± standard deviation. Difference between G1 and G2 were analyzed using Independent-Samples Students'*t*-test. One-Way Analysis of Variance was used to compare the means of G1 and G2 on the PNDs 70, 100, and 130. An overall $P \leq 0.05$ was considered statistically significant. The SPSS software package V16.1 (IBM Corporation, New York, NY, USA) was used for statistical analysis.

Results

Light microscopic examination

The light microscopic examination of the toluidine

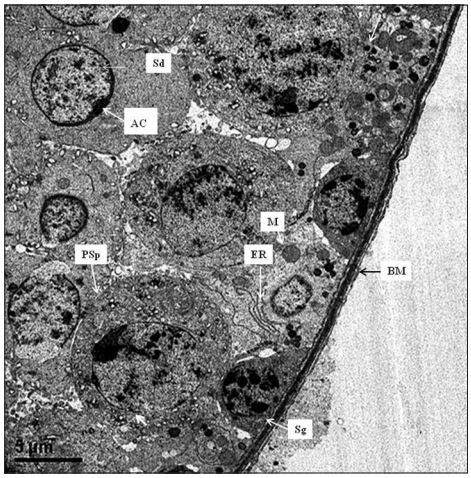

Figure 1: A transmission electron photomicrograph of an ultrathin section of a control rat's testis at 70 days showing basement membrane surrounding the seminiferous tubule. Sg: Spermatogonium, PSp: Primary spermatocyte, Sd: Spermatid, AC: Acrosomal cap, M: Mitochondria, ER: Endoplasmic reticulum. Scale bar-5 μm

blue-stained, semithin section of testis of the animals of G1 showed normal, regularly shaped STs and its epithelium [Figure 6a].

In G2, the rats at PND 70 had STs with different shapes and irregular outlines [Figure 6b]. Their stratified epithelium appeared disorganized. We observed vacuoles in the basal

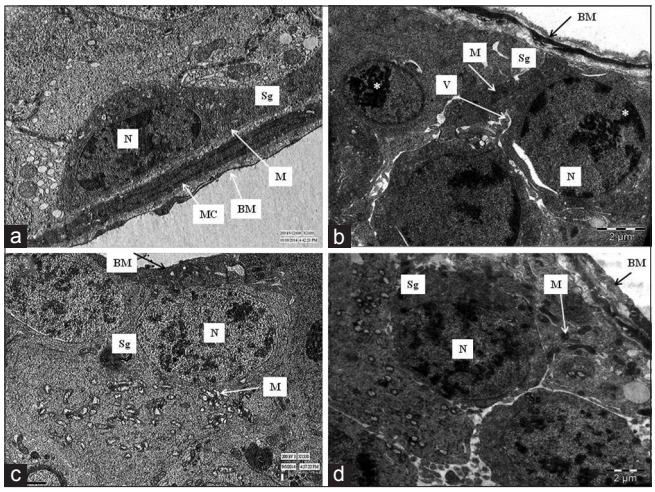

Figure 2: Transmission electron photomicrographs of ultrathin section of rat's testis showing spermatogonium lying on the basement membrane, with myoid cell with peripheral heterochromatin in nucleus (N) and normal mitochondria (M) in control group. (a); Sg having dense-clumped marginal chromatin material (*) in the nucleus (N) and vacuolation (V) in cytoplasm in phototherapy treated group at 70 days (b); Sg lying on irregular BM having distorted mitochondria (M) in phototherapy treated group at 100 days (c); with condensed heterochromatin in its nucleus (N) and normal appearing mitochondria in phototherapy treated group at 130 days (d). Scale bar: a = 1 µm; b = c = d = 2 µm

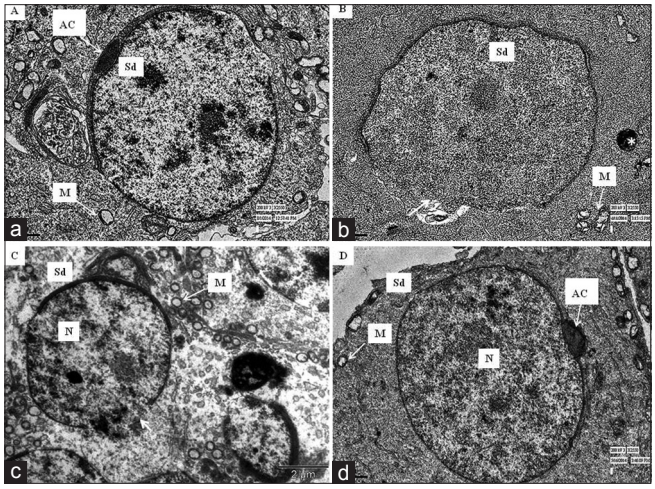

Figure 4: Transmission electron photomicrographs of ultrathin section of rat's testis showing spermatid containing large, rounded euchromatic nucleus (N), prominent Golgi apparatus (G) and acrosomal cap at one side of the nucleus and peripherally arranged mitochondria (M) in control group (a); spermatid having an irregular and damaged nuclear membrane (arrowheads), a few damaged mitochondria (M) and electron-dense material (*) in the cytoplasm in the phototherapy treated group at 70 days (b); spermatid with nuclear rupture (arrow), loss of cell boundary, and abnormal acrosome formation in the phototherapy treated group at 100 days (c); spermatid having normal euchromatic nucleus (N) and a prominent acrosomal cap in the phototherapy treated group at 130 days (d). Scale bar: a = b = d = 1 µm; c = 2 µm

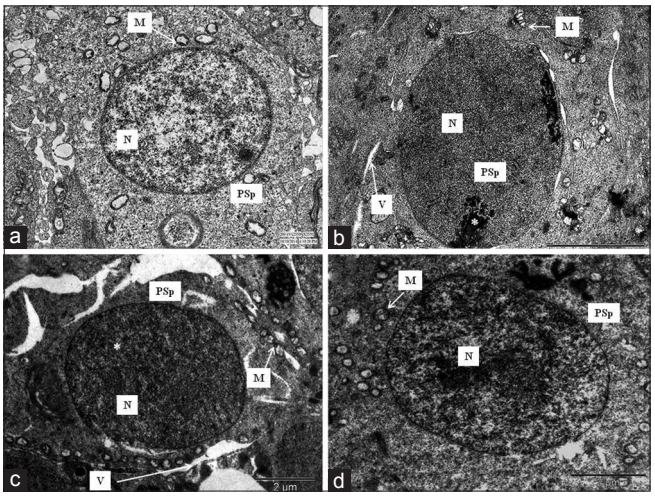

Figure 3: Transmission electron photomicrographs of ultrathin section of rat's testis showing primary spermatocyte with large, rounded nucleus (N) and ovoid mitochondria (M) in control group (a); PSp with clumped dense chromatin material (*) in the margins of the nucleus (N), cytoplasmic vacuoles (V), and swollen mitochondria (M) with irregular cristae in phototherapy treated group at 70 days (b); PSp with vacuoles in cytoplasm (V) and distorted mitochondria (M) with irregular cristae in phototherapy treated group at 100 days (c); the PSp appears as a large, rounded cell with round nucleus (N) containing clumps of heterochromatin scattered all over the nucleoplasm in phototherapy treated group at 130 days (d). Scale bar: A =1 µM; B = c = d = 2 µm

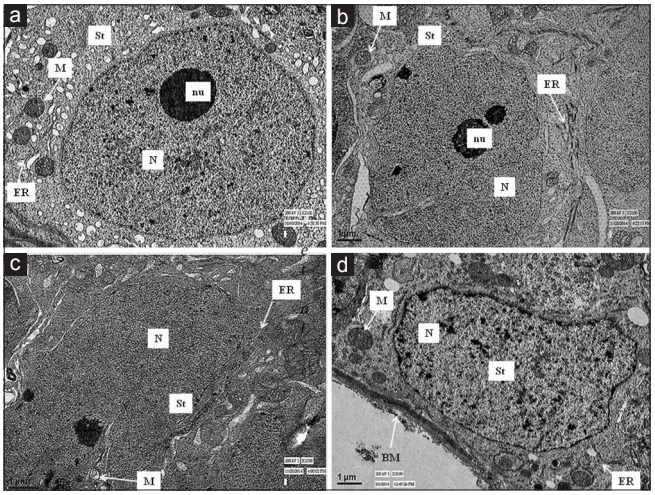

Figure 5: Transmission electron photomicrographs of ultrathin section of rat's testis showing Sertoli cells (St) with large euchromatic indented nucleus (N) with a prominent nucleolus (nu) and mitochondria (M) in control rat's testis (a); with irregular indented nucleus (N) and nucleolus (nu), dilated endoplasmic reticulum and M with irregular cristae in the phototherapy treated group at 70 days (b); having an irregular indented N, dilated ER in the phototherapy treated group at 100 days (c); appears with indented N with normal M and ER in phototherapy treated group at 130 days (d). BM: Basement membrane. Scale bar: a = b = c = d = 1 µm

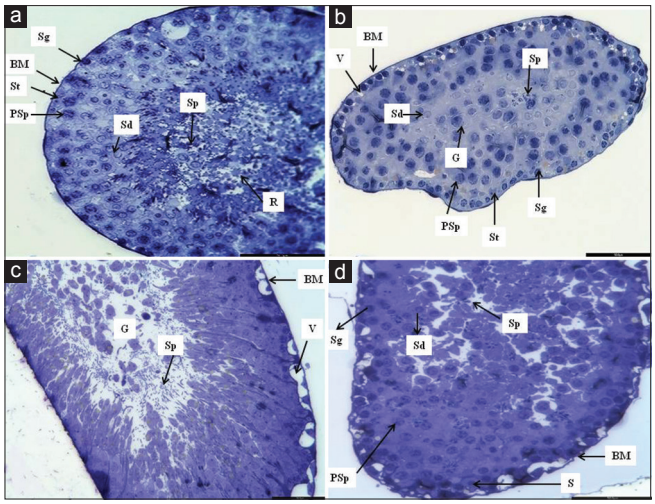

Figure 6: Photomicrographs of semithin section of rat's testis showing the lining epithelium of seminiferous tubules with normal arrangement of germinal epithelium in control group (a); seminiferous tubules with irregular outline, multiple V and G in lumen in the phototherapy treated group at 70 days (b); seminiferous tubules with disorganized germinal epithelium, abnormal spermatogenic cells and multiple V in the phototherapy treated group at 100 days (c); seminiferous tubules with germinal epithelium showing recovery toward normal architecture in the phototherapy treated group at 130 days (d). Sg: Spermatogonium, PSp: Primary spermatocyte, Sd: Spermatid, St: Sertoli cell, Sp: Sperms, R: Residual body, G: Exfoliated germ cells and V: Vacuole. Scale bar-50 μm

layer of the STs. Lumina of some STs contained very few spermatozoa and exfoliated germ cells [Figure 6b]. The testes on PND 100 showed STs with distorted BM, disorganized germinal epithelium and marked vacuolations in the cells. Lumina of STs contained sloughed and degenerated germ cells [Figure 6c]. In the testes on PND 130, we observed that the appearance of the ST epithelium was like those of G1 [Figure 6d].

Transmission electron microscopic examination

The testes of the animals of G1 revealed normal structure of the STs on PND 70, 100, and 130 [Figure 1].

In G2, the testes of PND 70 showed that the STs were surrounded by an irregularly thick and disrupted BM. Sg was seen lying on the BM and showed condensed, clumped peripheral heterochromatin. There were wide, intercellular spaces, and numerous intracellular vacuoles. The cytoplasm of the Sg often showed electron-dense bodies [Figure 2b]. Their mitochondria were swollen and had irregular cristae. Their SER appeared dilated [Figure 2b]. PSp showed irregular nuclear membrane, with dense, clumped chromatin material arranged at the nuclear periphery. Numerous cytoplasmic vacuoles were seen in the PSp [Figure 3b]. Most mitochondria in the PSp were swollen and showed irregular cristae. The SER in them was dilated. Sd also had disrupted nuclear membranes, swollen mitochondria with irregular cristae and dilated SER. Many of the mitochondria were seen closer to the nuclear membrane. Their AC formation appeared to be abnormal. Numerous electron-dense bodies were found in their cytoplasm [Figure 4b]. Sertoli cells had indented nuclei and showed prominent nucleoli within the nucleoplasm. Their cytoplasm also contained distorted mitochondria with irregular cristae. Their SER was also dilated in many regions [Figure 5b].

On PND 100, we saw that Sg with ill-defined boundaries rested on an irregular BM. Their nuclear membranes were often disrupted, and condensed heterochromatin was present in periphery of their nucleus. Their mitochondria were swollen, distorted, had few cristae and vacuoles [Figure 2c]. Most of the PSp had irregular and disrupted nuclear membrane. Their cytoplasm also had swollen, distorted mitochondria with irregular cristae. Their SER was dilated. Intracellular vacuoles and intercellular spaces were found in them [Figure 3c]. Most of the Sd appeared more damaged than G2 Sd cells at PND 70. Some of their nuclei showed abnormally dense and clumped chromatin and some Sd had ruptured nuclear membrane. Many mitochondria were found closer to the nuclear membrane. Swollen and irregular cristae were seen in some mitochondria. Their SER were dilated. Some Sd had electron-dense bodies in their nuclei and cytoplasm [Figure 4c]. Sertoli cells had indented nuclei. They also had distorted and swollen mitochondria with few cristae. Their SER was dilated and vacuolated.[Figure 5c].

The testis of the G2 animals on PND 130 showed that most STs had nearly normal architecture. Their BM appeared regular in outline and of uniform thickness. Their Sg had condensed heterochromatin in their nuclei resting near the BM. Their cytoplasm contained nearly normal mitochondria [Figure 2d]. The PSp appeared as large, rounded cells with large rounded nuclei containing clumps of heterochromatin scattered all over the nucleoplasm. They had a few vacuoles [Figure 3d]. The Sd had rounded euchromatic nuclei and a prominent AC. Their cytoplasm showed peripherally arranged normal-appearing mitochondria [Figure 4d]. Sertoli cell rested on a normal-looking BM and had indented nuclei. Their cytoplasm contained nearly normal-looking mitochondria [Figure 5d].

Discussion

In the present study, we found that Wistar rat pups that had been treated with conventional PT for 48 h after birth and sacrificed on PND 70 and 100, showed degenerative changes in the spermatogenic and Sertoli cells of their testes. However, on PND 130, the cells of the ST showed significantly lesser damage than on the previous days.

Five developmental time periods can be defined in the male rat on the basis of microscopic changes regarding PNDs: PND 0–7 (neonatal), PND 8–20 (infantile), PND 21–32 (juvenile), PND 33–55 (peri-pubertal), and PND 56–70 (late pubertal) periods.[12] At PND 70, male rats became sexually mature. Hence, we planned our study in a manner to verify if PT at birth affects the morphology of the testes at the time of attaining sexual maturity in rats.

With light microscopy, testes of animals of G2 on PND 70 showed damaged ST that had very few spermatozoa in their lumina. On PND 100, the distortion of the tubules and their cells were more marked and the lumina of STs contained numerous sloughed and degenerated cells. Under stressed conditions, the spermatogenic cells become loosely arranged and get off in the lumina of STs due to retraction of apical and lateral processes of Sertoli cells which are present between stratified layer of germ cells.[13] Further, the accumulation of degenerated germ cells in the lumina of ST seen in our study may be due to the malfunction of the affected Sertoli cells to engulf these damaged cell bodies.[14]

Ultrastructurally, the testes of rats of G2 on PND 70 and 100 showed evidence of increased intercellular spaces between the various components of the ST, indicative of tubular edema. It has been shown that injury caused by heavy metals such as Pb and cadmium can disrupt intercellular junctional complexes and may cause ischemia and necrosis of the testes leading to increase in intercellular spaces.[15] Conventional PT also produces changes that are like those seen in animals exposed to Cd and Pb.

In the present study, STs on PND 70 of the G2 rats showed an irregularly thick wall [Figures 6b and 2b]. This thickening may be due to increase in the amount of collagenous fibers in STW and the number of myoid cells in the lamina propria of the ST. The amount of collagen fibers may be increased by two processes either due to an increased production of collagen fibers by fibroblasts or a decreased rate of collagen phagocytosis.[16] Further, the irregularities in the tubular wall, observed in the present study might be due to either tubular shrinkage or contraction of myoid cells.[14] For the proper release of spermatozoa from the Sertoli cells into the lumen of STs, ratio of collagen fibers and myoid cells should be maintained.[17] Due to change in proportion of these, only few spermatozoa were found in the lumen of ST on PND 70, in our study. It may be possible that the process of healing commences well before PND 100 and 130. This may be the reason why we saw a decrease in tubular wall damage at these time points.

In this present study, spermatogenic cells and Sertoli cells of G2 showed mitochondrial damage that was evidenced by their swelling and the presence of irregular cristae. These changes may be due to excessive production of reactive oxygen species (ROS). PT activates i the release of reactive nitrogen species and ROS which are cytotoxic and genotoxic[18,19] ROS can be produced when visible light excites cellular photosensitizers. In nonpigmented cells, flavin-containing oxidases in mitochondria and peroxisomes are well known photosensitizers that are activated by the photoreduction of flavins by violet-blue light. Activation of flavin-containing oxidases in mitochondria leads to the generation of hydrogen peroxide (H_2O_2), which is responsible for ROS formation.[20] The ROS causes alteration in selective permeability of the inner membrane of mitochondria, which is called mitochondrial permeability transition (MPT). MPT is responsible for swelling of the mitochondrial matrix,[21,22] After swelling of the intermembrane space, the outer membrane ruptures due to less distension capacity of the outer membrane.[23] Due to this surface area of the inner mitochondrial membrane is increased which leads to the unfolding in the cristae.[24] This may explain the swollen mitochondria and irregular cristae seen in our study [Figure 3b and d]. The high levels of ROS can attack biological molecules such as phospholipids, DNA, and proteins.[25] This may explain the disruption of the nuclear membrane and dilated endoplasmic reticulum (ER) seen in many spermatogenic and Sertoli cells, seen in our study [Figures 4b, 5b and c].

Further, Sertoli cells of the animals of G2 showed vacuoles in the cytoplasm. One of the early and most common morphological features of damage to the testis is vacuolations of Sertoli cells.[26] These might have formed due to the autophagosomes formed for the phagocytosis of necrotic germ cells by Sertoli cells.[11,27] Another reason for the vacuolization of Sertoli cells may be due to swelling and coalescence of intracellular membrane-bound organelles like the ER.[28]

In the present study, spermatogenic cells showed degeneration. This might be either due to direct damage to these spermatogenic cells caused by ROS, generated either during PT or secondary to the injury to the Sertoli cells. Sertoli cells play an important role in spermatogenesis. Sertoli cells produce lactate, which is important for the survival of germ cell.[28] Any injury to Sertoli cells would affect the nutrition and sustenance of spermatogenic cells and Pb to their disintegration, subsequent necrosis, and their exfoliation into the lumen of the ST.[26] In addition, the separation of spermatogenic cells from Sertoli cells due to intercellular edema, as we have observed in this study, would prevent the transfer of nutrients from Sertoli cells to the spermatogenic cells.

The ROS production and the damage to the mitochondrial permeability may also be responsible for the increase in mean mitochondrial diameter of all germ cells at PND 70; wherein, we observed the maximum mitochondrial diameter of spermatogenic cells. This may be due to swelling of the mitochondria. The process of recovery may explain the decrease in mitochondrial diameter on the 100th and 130th PND. However, we noticed an increase in mitochondrial diameter of spermatogenic cells in animals of G1. However, at all points, their mitochondrial diameters were lower than those observed in G2 [Table 1]. Hence, we conclude that there may be an increase in the size of mitochondria that comes with age and maturity of the ST.

Degeneration of spermatogenic cells in our study might be due to either direct damage to these spermatogenic cells caused by ROS or secondary to the injury to the aertoli cells. Sertoli cells play an important role in spermatogenesis and produce lactate, which is important for spermatogenic germ cells survival,[26,28] In addition, the separation of Sd and spermatocytes from Sertoli cells due to intercellular edema, as we have observed in this study would interfere with the transfer of nutrients from Sertoli cells.

Table 1: Comparison of seminiferous tubular wall thickness, spermatogonia mitochondrial diameter, primary spermatocytes mitochondrial diameter, and spermatids mitochondrial diameter between Groups I and II

Postnatal days	Mean±SD							
	STWT (μm)		SGMD (μm)		PSMD (μm)		SMD (μm)	
	GI (*n*=18)	GII (*n*=18)	GI (*n*=18)	GII (*n*=18)	GI (*n*=18)	GII (*n*=18)	GI (*n*=18)	GII (*n*=18)
70-days (*n*=6)	0.953±0.065	1.121±0.179$^{@}$	0.395±0.069	0.603±0.152$^{@}$	0.241±0.025	0.377±0.112$^{@}$	0.260±0.045	0.449±0.084$^{@}$
100-days (*n*=6)	0.981±0.057	0.896±0.088*	0.429±0.057	0.483±0.112*	0.280±0.059	0.351±0.076$^{\#}$	0.273±0.046	0.360±0.051*
130-days (*n*=6)	0.996±0.199	0.727±0.097$^{@}$	0.419±0.053	0.442±0.097*	0.306±0.061	0.328±0.037$^{\#}$	0.289±0.070	0.283±0.052$^{@}$

*$P\leq0.05$: Significant; $^{\#}P<0.01$: Highly Significant; $^{@}P<0.001$: Very highly significant. SD: Standard Deviation; PND: Postnatal day, STWT: Seminiferous tubular wall thickness, SGMD: Spermatogonia mitochondrial diameter, PSMD: Primary spermatocytes mitochondrial diameter, SMD: Spermatids mitochondrial diameter

As we have discussed above, the damage to the mitochondria leads to the exposure of their inner membrane, which causes the release of mitochondrial intermembrane space proteins such as cytochrome c, apoptosis-inducing factor and endonuclease G.[29] They ultimately initiate apoptosis and may be responsible for spermatogenic cell death through the caspase-dependent and independent apoptotic pathway.[30] This also explains the features of apoptosis such as condensation and margination of the chromatin material and features of mitochondrial damage. There are other studies that have also reported a significant increase of apoptosis caused by PT. It has also been shown that PT can induce apoptosis in lymphoma cell lines,[8] in peripheral blood lymphocytes of infants,[18] and in neonatal small intestine.[9] It has also been seen that PT causes an additive effect on DNA damage in newborn with jaundice.[31] Furthermore, Koç *et al*. (1999) reported that PT causes degenerative changes in the rat's testes, however, they did not observe any changes in fertilization rates.

We observed that Sg and Sertoli cells showed clear signs of having started recovering from the PT-induced damage on PND 130. It has been shown before that spermatogenesis may recover if adequate time is given for replication of the stem cell SG to replenish their numbers, although the differentiating Sg are depleted.[26]

Conclusions

The present study shows that conventional PT exposure for 48-hin newborn Wistar rat pups caused degenerative ultrastructural changes of the ST, that were prominently seen at PND 70 and 100; however, by the PND 130, these cells showed signs of recovery to their almost normal architecture. Therefore, newborn infants, who receive PT, need to be investigated for reproductive function around puberty.

Financial support and sponsorship

Nil.

Conflicts of interest

There are no conflicts of interest.

References

1. Usatin D, Liljestrand P, Kuzniewicz MW, Escobar GJ, Newman TB. Effect of neonatal jaundice and phototherapy on the frequency of first-year outpatient visits. Pediatrics 2010;125:729-34.
2. Dennery PA, Seidman DS, Stevenson DK. Neonatal hyperbilirubinemia. N Engl J Med 2001;344:581-90.
3. Maisels MJ, McDonagh AF. Phototherapy for neonatal jaundice. N Engl J Med 2008;358:920-8.
4. Yahia S, Shabaan AE, Gouida M, El-Ghanam D, Eldegla H, El-Bakary A, *et al.* Influence of hyperbilirubinemia and phototherapy on markers of genotoxicity and apoptosis in full-term infants. Eur J Pediatr 2015;174:459-64.
5. Tan KL. Phototherapy for neonatal jaundice. Clin Perinatol 1991;18:423-39.
6. Koç H, Altunhan H, Dilsiz A, Kaymakçi A, Duman S, Oran B, *et al.* Testicular changes in newborn rats exposed to phototherapy. Pediatr Dev Pathol 1999;2:333-6.
7. Cetinkursun S, Demirbag S, Cincik M, Baykal B, Gunal A. Effects of phototherapy on newborn rat testicles. Arch Androl 2006;52:61-70.
8. Roll EB. Bilirubin-induced cell death during continuous and intermittent phototherapy and in the dark. Acta Paediatr 2005;94:1437-42.
9. Tanaka K, Hashimoto H, Tachibana T, Ishikawa H, Ohki T. Apoptosis in the small intestine of neonatal rat using blue light-emitting diode devices and conventional halogen-quartz devices in phototherapy. Pediatr Surg Int 2008;24:837-42.
10. Campion SN, Carvallo FR, Chapin RE, Nowland WS, Beauchamp D, Jamon R, *et al.* Comparative assessment of the timing of sexual maturation in male Wistar Han and Sprague-Dawley rats. Reprod Toxicol 2013;38:16-24.
11. Wahbah NS, El-Fattah EA, Ahmed FE, Hassan EZ. Histological study of the effect of exogenous glucocorticoids on the testis of prepubertal albino rat. Egypt J Histol 2010;33:353-64.
12. Picut CA, Remick AK, de Rijk EP, Simons ML, Stump DG, Parker GA, *et al.* Postnatal development of the testis in the rat: Morphologic study and correlation of morphology to neuroendocrine parameters. Toxicol Pathol 2015;43:326-42.
13. Rai J, Pandey SN, Srivastava RK. Effect of immobilization stress on spermatogenesis of albino rats. J Anat Soc India 2003;52:55-7.
14. Mohamed D, Saber A, Omar A, Soliman A. Effect of cadmium on the testes of adult albino rats and the ameliorating effect of zinc and Vitamin E. Br J Sci 2014;11:72-95.
15. Bizarro P, Acevedo S, Niño-Cabrera G, Mussali-Galante P, Pasos F, Avila-Costa MR, *et al.* Ultrastructural modifications in the mitochondrion of mouse Sertoli cells after inhalation of lead, cadmium or lead-cadmium mixture. Reprod Toxicol 2003;17:561-6.
16. Makhlouf M, Eldin MS, Zagloul AM. The effect of lead acetate on testicular structure and protective effect of Vitamin E in adult albino rat. Egypt J Histol 2008;31:406-18.
17. Aydos K, Güven MC, Can B, Ergün A. Nicotine toxicity to the ultrastructure of the testis in rats. BJU Int 2001;88:622-6.
18. Yahia S, Shabaan AE, Gouida M, El-Ghanam D, Eldegla H, El-Bakary A, *et al.* Influence of hyperbilirubinemia and phototherapy on markers of genotoxicity and apoptosis in full-term infants. Eur J Pediatr 2015;174:459-64.
19. Christensen T, Kinn G, Granli T, Amundsen I. Cells, bilirubin and light: Formation of bilirubin photoproducts and cellular damage at defined wavelengths. Acta Paediatr 1994;83:7-12.

20. Godley BF, Shamsi FA, Liang FQ, Jarrett SG, Davies S, Boulton M, *et al.* Blue light induces mitochondrial DNA damage and free radical production in epithelial cells. J Biol Chem 2005;280:21061-6.
21. Petit PX, Lecoeur H, Zorn E, Dauguet C, Mignotte B, Gougeon ML, *et al.* Alterations in mitochondrial structure and function are early events of dexamethasone-induced thymocyte apoptosis. J Cell Biol 1995;130:157-67.
22. Petit PX, Susin SA, Zamzami N, Mignotte B, Kroemer G. Mitochondria and programmed cell death: Back to the future. FEBS Lett 1996;396:7-13.
23. Sesso A, Belizário JE, Marques MM, Higuchi ML, Schumacher RI, Colquhoun A, *et al.* Mitochondrial swelling and incipient outer membrane rupture in preapoptotic and apoptotic cells. Anat Rec (Hoboken) 2012;295:1647-59.
24. Scorrano L, Ashiya M, Buttle K, Weiler S, Oakes SA, Mannella CA, *et al*. A distinct pathway remodels mitochondrial cristae and mobilizes cytochrome c during apoptosis. Dev Cell 2002;2:55-67.
25. Mayne ST. Antioxidant nutrients and chronic disease: Use of biomarkers of exposure and oxidative stress status in epidemiologic research. J Nutr 2003;133:933-40.
26. Creasy DM. Pathogenesis of male reproductive toxicity. Toxicol Pathol 2001;29:64-76.
27. Wang H, Wang H, Xiong W, Chen Y, Ma Q, Ma J, *et al.* Evaluation on the phagocytosis of apoptotic spermatogenic cells by Sertoli cells *in vitro* through detecting lipid droplet formation by oil red O staining. Reproduction 2006;132:485-92.
28. Hild SA, Reel JR, Dykstra MJ, Mann PC, Marshall GR. Acute adverse effects of the indenopyridine CDB-4022 on the ultrastructure of Sertoli cells, spermatocytes, and spermatids in rat testes: Comparison to the known Sertoli cell toxicant di-n-pentylphthalate (DPP). J Androl 2007;28:621-9.
29. Tsujimoto Y, Shimizu S. Role of the mitochondrial membrane permeability transition in cell death. Apoptosis 2007;12:835-40.
30. van Gurp M, Festjens N, van Loo G, Saelens X, Vandenabeele P. Mitochondrial intermembrane proteins in cell death. Biochem Biophys Res Commun 2003;304:487-97.
31. El-Abdin MY, El-Salam MA, Ibrhim MY, Koraa SS, Mahmoud E. Phototherapy and DNA changes in full-term neonates with hyperbilirubinemia. Egypt J Med Hum Genet 2012;13:29-35.